Time-resolved Coulomb explosion imaging: A method to measure structure and dynamics of molecular nuclear wave packets

Henrik Stapelfeldt,[1,*] Eric Constant,[1,2†] Hirofumi Sakai,[1,3] and Paul B. Corkum[1]
[1]*Steacie Institute for Molecular Sciences, National Research Council of Canada, Ottawa, Ontario, Canada K1A 0R6*
[2]*Département de Physique, Faculté des Sciences, Université de Sherbrooke, Sherbrooke, Québec, Canada J1K 2R1*
[3]*Electrotechnical Laboratory, 1-1-4, Umezono, Tsukuba, Ibaraki 305, Japan*
(Received 20 August 1997; revised manuscript received 22 January 1998)

Coulomb explosion of molecules induced by an intense femtosecond probe laser pulse provides an approach to measure structure and dynamics of internuclear wave packets on a natural spatial (Å) and temporal (fs) scale for molecules. The technique is illustrated by applying it to study photodissociation of I_2 initiated by a femtosecond pump pulse. We report a resolution of ~2–4 Å in the internuclear range ~7–14 Å using an 80-fs probe pulse. We discuss the ultimate spatial and temporal resolution of the technique, as well as the possibilities of observing dynamics of dissociating polyatomic molecules. Intense femtosecond laser pulses not only provide a way of probing molecular dynamics but they are also an efficient means to initiate dynamics in, e.g., molecular ionic states. [S1050-2947(98)10106-3]

PACS number(s): 33.80.Rv, 34.50.Gb, 82.50.Fv

I. INTRODUCTION

Femtosecond time-resolved studies of ultrafast phenomena in condensed media or in gases are of great interest in chemistry, physics, and biology [1]. In such studies the main technique applied is pump-probe spectroscopy where a femtosecond laser pulse initiates an event of interest and the subsequent evolution is followed by probing the system with another, temporally delayed, femtosecond pulse. In both condensed phase and gas phase, there is rarely more than one photon used for either the pump step or the probe step since additional photons usually add extra complexity, thereby making the interpretation of the experimental results more difficult.

A different approach to femtosecond (fs) pump-probe measurements of molecules in the gas phase is now possible [2]. For this approach perturbation theory is abandoned in the probe step and in some cases also in the pump step. It relies on the fact that there are usually two simple limits in the interaction between light and matter. The first one is the widely used perturbation limit in which one or a few photons are involved. The second one is the strong field limit in which a very large number of photons participate. Recent research in atomic and molecular physics shows that ionization induced by intense laser pulses of short duration can be understood by quasistatic or tunneling models [3,4] that are as simple and intuitive as perturbation theory. Pump-probe experiments in the strong-field limit are virtually unexplored but they have the potential to lead to new insight since studies in this extreme are unrelated to the Fourier transform of traditional frequency-resolved spectroscopic methods.

In this paper we concentrate on the many-photon limit and demonstrate how an intense probe pulse can be used to measure structure and dynamics of molecules by time-resolved Coulomb explosions. Coulomb explosions of molecules following the collision between a fast molecular beam and a thin foil is used to obtain information about molecular structure [5,6]. Here, we use an intense femtosecond laser pulse rather than a thin foil to induce the Coulomb explosion. Even though the interaction time between the intense laser pulse and the molecule (equal to the pulse duration) is significantly longer than the transit time of a molecular ion through the foil ($\leqslant$1 fs), it is still short enough to essentially freeze the nuclear motion during ionization. Furthermore, in contrast to the foil method, the laser-induced approach allows us to follow the temporal evolution of the molecular structure with a time resolution determined by the duration of the laser pulses.

Recently, we reported the first work on femtosecond time-resolved laser-induced Coulomb explosions in which photodissociation of I_2 molecules was measured [7]. The basic idea of the technique is the following. First, an 80-fs [full width at half maximum (FWHM)], linearly polarized, 625-nm laser pulse excites a coherent superposition of continuum states (a dissociative wave packet) by a single-photon transition from the $X\ ^1\Sigma_g^+$ potential to the $A\ ^3\Pi_{1u}$ potential (Fig. 1). Second, the wave packet moves along the $A\ ^3\Pi_{1u}$ potential curve with an asymptotic internuclear velocity of ~11.6 Å/ps. Third, the position and the structure of the wave packet is determined by exposing the molecule to an intense, 80-fs, temporally delayed, laser pulse. This causes rapid ejection of several electrons from the molecule corresponding to a quasi-instantaneous projection of the wave packet on a repulsive Coulombic state of a multiply charged molecular ion. The Coulomb repulsion between the resulting atomic ions gives rise to the Coulomb explosion. The internuclear distance of the molecule, before the irradiation with the probe pulse, can be determined by measuring the Coulomb energy, released as kinetic energy of the atomic ions since the internuclear distance does not change during the removal

*Permanent address: Department of Chemistry, Aarhus University, Langelandsgade 140, DK-8000 Aarhus C, Denmark.
†Permanent address: CPMOH, Universite Bordeaux 1, 351 Cours de la Liberation, F-33 405 Talence, France.

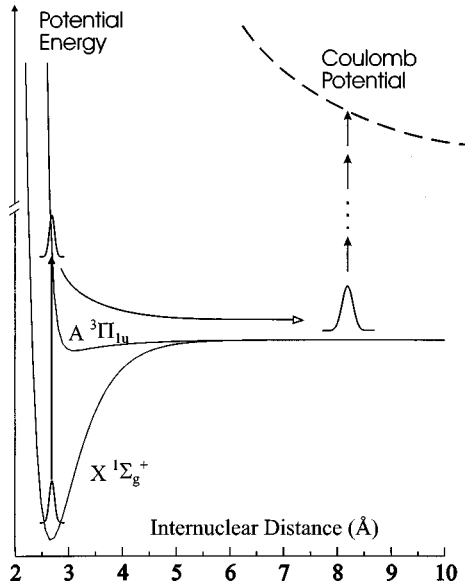

FIG. 1. A schematic of selected potential curves of I_2 illustrating the formation of the $A\ ^3\Pi_{1u}$ wave packet and its subsequent projection by multiphoton ionization onto a repulsive Coulomb potential.

of the electrons. Furthermore, the distribution of kinetic energies determines the structure of the internuclear wave packet.

The paper is organized in the following way. After a description of the experimental technique in Sec. II we present our experimental results for the photodissociation of I_2 consisting of kinetic energy spectra measured at different delays between the pump and the probe pulse (Sec. III). We explain how these spectra enable us to determine the square of the internuclear wave function at different times after the excitation of the wave packet with a resolution of ~2–4 Å in the internuclear range 7–14 Å. A usual concern in femtosecond experiments is nonlinear effects induced by the pump laser. In Sec. IV we discuss how they influence our experimental results. We also discuss how it should be possible to use nonlinear interactions to initiate dynamics in, e.g., molecular ionic states. Section V deals with the present limitations due to space charge effects, and in Sec. VI we discuss the ultimate spatial resolution for the Coulomb explosion method. In the last section before the summary we discuss how the technique might be applied to study molecular dynamics in the regime of smaller internuclear separations, and we mention the possibilities of extending our approach from diatomic to polyatomic molecules (Sec. VII).

II. EXPERIMENTAL TECHNIQUE

A schematic of the experimental setup is shown in Fig. 2. An amplified colliding pulse modelocked (CPM) laser provides 80-fs-long (FWHM of a Gaussian fit) pulses with a pulse energy of ~250 μJ. The wavelength is centered around 625 nm, the bandwidth is ~32 meV (FWHM of a Gaussian fit), and the repetition rate is 10 Hz. The output pulse of the laser system is split in a Michelson arrangement introducing a controllable delay between the pump and the probe pulse. The relative intensity of the two pulses is controlled by using a partially reflecting mirror in one of the arms (typical reflectivity ~30%). The zero delay is determined by cross correlation in a 100-μm-thick KDP crystal. The two beams are focused by an $f=1.5$ m lens through a 500-μm pinhole, which ensures good spatial overlap of the two beams. The pinhole is imaged with a 5-cm-focal-length on-axis parabolic mirror to a focal spot diameter of ~25 μm inside an ultrahigh vacuum (UHV) chamber. Typically, the pump and the probe pulses have peak intensities of $\sim 3\times10^{13}$ W/cm^2 and $\sim 9\times10^{13}$ W/cm^2, respectively.

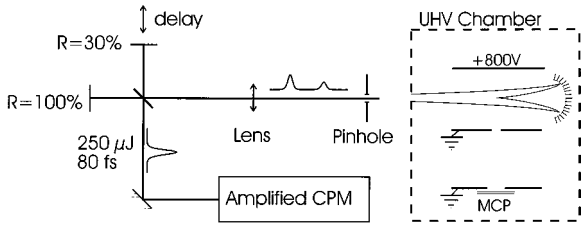

FIG. 2. A schematic of the experimental setup showing the Michelson arrangement and the UHV chamber. The molecular beam propagates perpendicular to the plane of the paper.

A pulsed beam of molecular iodine seeded in helium, formed by expanding 0.3 Torr I_2 in 750 Torr He through a ~250-μm-diameter stainless steel nozzle, crosses the laser beams 8 cm away from the nozzle. In the present experiment we do not measure the rotational temperature, $T_{\rm rot}$, or the vibrational temperature, $T_{\rm vib}$, but laser-induced fluorescence studies of supersonic expansion of I_2 under virtually identical experimental conditions [8] yielded $T_{\rm rot}\leqslant 10$ K and $T_{\rm vib}\leqslant 200$ K. A vibrational temperature of ~200 K corresponds to a Boltzman distribution with 78% of the I_2 molecules in the $\nu=0$ vibrational level, 17% in the $\nu=1$ level, and 4% in the $\nu=2$ level. The density of I_2 molecules in the laser focus can be estimated by an analytical expression assuming an ideal free-jet expansion [9]. The result, 6×10^{10} molecules per cm^3, is likely an overestimate, but indicates that the actual density is as high as 10^{10} cm^{-3}.

The ions produced from the probe laser irradiation are analyzed in a time-of-flight (TOF) spectrometer [10] that is oriented perpendicular to both the molecular beam and the laser beams. It consists of an accelerating (electric field ~267 V/cm) and a field-free drift zone equipped with a dual-microchannel-plate detector at the end. Time-of-flight spectra are recorded using a digital oscilloscope with a sampling rate of 10^9 per second and an analog bandwidth of 500 MHz. The flight time of any ion is a measure of its mass-to-charge ratio and its initial velocity along the TOF axis. A 0.5-mm aperture and a 1-mm-wide slit at the exits of the accelerating and the drift region ensure that we only observe fragments with their velocity vector essentially aligned with the TOF axis. Since the measured velocity almost equals the total velocity, the kinetic energy $E_{\rm kin}$ of the ions can be determined. Also, the aperture and the slit ensure that we can control the polarization of the laser beams with respect to the internuclear axis of those molecules that are detected. The size of the aperture and the slit and the magnitude of the electric field in the accelerating zone define the acceptance angle (the maximum angle between the TOF axis and the velocity vector of a detected fragment) and the energy resolution of the spectrometer. The acceptance angle scales as $1/\sqrt{E_{\rm kin}}$ and is 9.6° for an I^+ ion with an initial kinetic energy of 1 eV. As

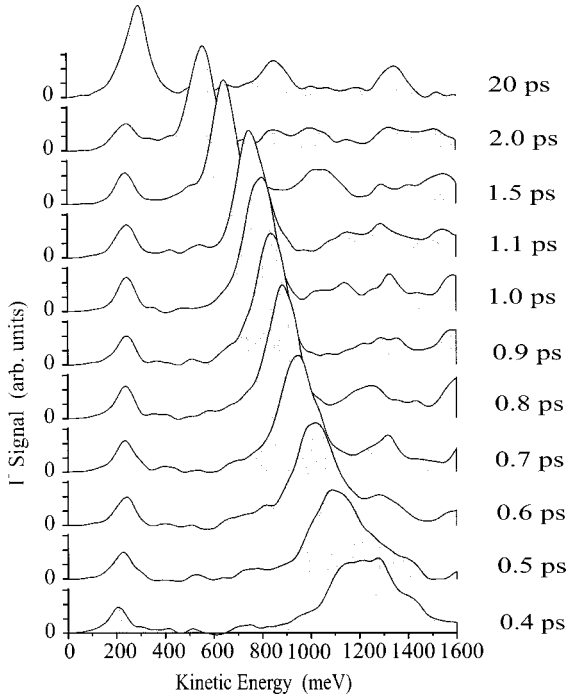

FIG. 3. Kinetic energy spectra of I^+ recorded at different delays between the pump and the probe laser pulse. The spectra are corrected for the dependence of the collection efficiency on the kinetic energy. Each spectrum is an average of 1000 laser shots.

a consequence, the collection efficiency of specific fragments is inversely proportional to their kinetic energy in good agreement with our observations. Finally, the energy resolution of the TOF spectrometer causes a broadening of ~30 meV towards lower energies for I^+ ions independent of their kinetic energy.

III. EXPERIMENTAL RESULTS

In Fig. 3 we show the kinetic energy spectra of the I^+ ions at different delays between the pump and the probe pulses. The pump pulse is polarized perpendicular to the TOF axis. This ensures that molecules aligned parallel to the TOF axis, which are the ones that will contribute to the I^+ signal (due to the directional selectivity of the ion spectrometer), can be excited to the dissociative $A\ ^3\Pi_{1u}$ potential since the $X\ ^1\Sigma_g^+ \rightarrow A\ ^3\Pi_{1u}$ transition is perpendicular [11]. The probe pulse is also polarized perpendicular to the TOF axis. This serves to minimize the ''background'' signal produced when the probe pulse multiple ionizes those molecules that were not excited by the pump pulse. The multiple ionization of the I_2 ground-state molecules leads, among other things, to the formation of I^+ ions with high kinetic energy ($\geq$1 eV). These ions are ejected in a narrow cone around the direction of the polarization of the probe laser [10], and therefore they do not contribute to the detected I^+ signal because of the directional discrimination imposed by the apertures in the spectrometer. Also, metastable I_2^{2+} ions (same mass-to-charge ratio as I^+ ions) are formed. They give rise to a sharp peak in the center of the I^+ part of the TOF spectrum corresponding to the section where very low energy I^+ fragments would appear ($\leq$25 meV). Although the background is minimal, we still correct our spectra recorded with both the pump and the probe pulse by subtracting a spectrum recorded with only the probe pulse.

There is a second reason for keeping the probe pulse polarized perpendicular to the TOF axis. Since we only observe molecules with the internuclear axis parallel to the TOF axis, the choice of perpendicular polarization of the probe pulse ensures that all observed molecules have their internuclear axis perpendicular to the electric field of the probe pulse. In this case the ionization rate induced by the probe pulse is virtually independent of the internuclear separation R of the dissociating molecule [4,12].

Two prominent peaks are observed in the spectra (Fig. 3). The position of the peak at ~240 meV is independent of the time difference between the pump and the probe pulse and therefore of the wave packet's internuclear separation. Consequently, it must result from the wave packet being projected on an I^+-I potential curve since any such curve is expected to be flat for the internuclear distances considered here (at 0.4 ps the internuclear distance should be already ~7 Å). Thus, this peak reflects the distribution of dissociation energies of the wave packet moving on the $A\ ^3\Pi_{1u}$ potential.

The large peaks at higher kinetic energies are due to projection of the wave packet on an I^+-I^+ potential curve. As the time delay is increased the I^+-I^+ peak moves toward lower kinetic energies corresponding to Coulomb exploding molecules with larger and larger internuclear separation. At a delay of 20 ps (uppermost trace) the I^+-I^+ peak almost coincides with the I^+-I peak, indicating that the internuclear distance of the dissociating molecule is so large that very little kinetic energy is released when the intense probe pulse ionizes the two widely separated iodine atoms.

The observation of two peaks in the I^+ spectrum is exactly what is expected in ionization experiments of dissociating diatomic molecules [13]. If the intensity in a certain part of the laser focus is sufficiently high that the ionization probability of the iodine atom is large, then it is most likely that both iodine atoms are ionized (projection of the wave packet onto an I^+-I^+ potential). In lower-intensity regions it is possible that only one of the two iodine atoms is ionized (projection onto an I^+-I potential). The observed ratio of the I^+-I^+ and I^+-I shows that the peak intensity of the probe pulse is high enough to cause ionization of both iodine atoms in most regions of the focus.

We now discuss how the kinetic energy distribution of the I^+-I^+ peaks in Fig. 3 can be used to determine the distribution of internuclear distances of the wave packet. The kinetic energy E_{kin} of an I^+ ion originating from fragmentation of an I^+-I^+ state is the sum of the energy from the dissociation E_{dis} on the initial $A\ ^3\Pi_{1u}$ potential and the energy released from the Coulomb explosion E_{Coul} of the I^+-I^+ state:

$$E_{\mathrm{kin}} = E_{\mathrm{dis}} + E_{\mathrm{Coul}}. \tag{1}$$

Assuming that the laser pulse used for exciting the wave packet is transform limited [14], the kinetic energy distribution $P(E_{\mathrm{kin}})$ is given by

$$P(E_{\mathrm{kin}}) = \int P(E_{\mathrm{dis}}) P(E_{\mathrm{Coul}} = E_{\mathrm{kin}} - E_{\mathrm{dis}}) dE_{\mathrm{dis}}, \tag{2}$$

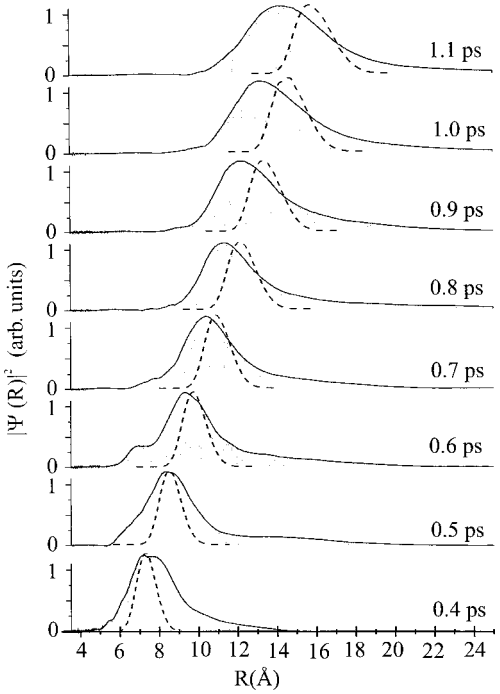

FIG. 4. The square of the internuclear wave function, $|\Psi(R)|^2$, of the dissociating I_2 molecule measured at different times after excitation by the pump pulse. The full curves are the measurements based on the kinetic energy spectra in Fig. 3. The broken curves represent a simulation of the wave packet motion on the $A\ ^3\Pi_{1u}$ potential (see text). The amplitudes of the simulated wave packets are scaled to match the observations.

where $P(E_{\rm dis})$ and $P(E_{\rm Coul})$ denote the probability distribution of the dissociation energy and the Coulomb energy, respectively. Since $P(E_{\rm kin})$ and $P(E_{\rm dis})$ are determined by the I^+-I^+ and the I^+-I, respectively, $P(E_{\rm Coul})$ can be extracted by deconvolving the two signals. The distribution of internuclear distances, $P(R)$, is now easily found from $P(E_{\rm Coul})$ since $E_{\rm Coul}$ and R are related via

$$E_{\rm Coul}=\frac{1}{2}\,\frac{qq'e^2}{4\pi\varepsilon_0 R} \tag{3}$$

(Coulomb's law), where q and q' are the charge states of the fragmented ions. In the case of the I^+-I^+ channel $q=q'=1$, Eq. (3) can be written as

$$R(\text{Å})=7200/E_{\rm Coul}(\text{meV}). \tag{4}$$

In Fig. 4 we show the results of the deconvolution—that is, the distribution of internuclear separations of the dissociating molecule at different times after excitation. The figure illustrates how the wave packet moves from an internuclear separation of ~7 Å to ~14 Å with a constant internuclear velocity. The width of the wave packet is 2–4 Å for the internuclear separations shown here.

Also shown in Fig. 4 is a classical simulation of the wave packet motion (broken curves). The simulation is based on propagating a wave packet excited by an 80-fs (FWHM) Gaussian pulse on the $A\ ^3\Pi_{1u}$ potential curve. We use an existing analytical expression for the $A\ ^3\Pi_{1u}$ potential derived from spectroscopic studies [15,16], and the distribution of dissociation energies is modeled by a functional form of the distribution as determined from the I^+-I signal (see Sec. IV B).

There are two important points to note in the comparison between the experimental results and the simulation. First, the observed wave packet appears to move slower than expected from the calculation and, second, the structure of the experimentally determined wave packet is significantly broader than the wave packet obtained from the simulation. Several physical phenomena that may be responsible for the discrepancies between the simulations and the measurements are discussed in the next three sections. These include nonlinear effects in the pump step due to the relative high intensity of the pump pulse (Sec. IV), space charge effects caused by a high charge density in the laser focus after irradiation of the molecules by the probe pulse (Sec. V), the finite duration of the probe pulse, which imposes the ultimate spatial resolution (Sec. VI). In addition, the limited resolution of the ion spectrometer causes a broadening of the internuclear probability density of the wave packet towards large R values. This is briefly mentioned in Sec. VI.

IV. NONLINEAR EFFECTS IN THE FORMATION OF THE WAVE PACKET

A. Multiphoton excited wave packets

In order to obtain a high transition rate in the single photon process that forms the wave packet, the fluence of the pump pulse must be high. However, this inevitably leads to high intensity of the pump pulse due to its short duration. Nonlinear effects due to the pump pulse should always be a concern in femtosecond experiments. At the intensity of the pump pulse employed in our experiment ($\sim 3\times10^{13}$ W/cm^2), the I_2 molecules are likely excited not just to the $A\ ^3\Pi_{1u}$ potential by one-photon absorption but also to higher-lying potential curves by multiphoton absorption [17]. In general, this will lead to dissociation via different potential curves and therefore to creation of several different wave packets.

Experimentally, multiphoton excitation is revealed by recording spectra at very large time delays. Here, the Coulomb energy released is very small and the energy of the peaks in the kinetic energy spectra is almost equal to the dissociation energy of the wave packet. In the 20-ps spectrum of Fig. 3, two peaks, at energies of ~840 and ~1320 meV, are observed in addition to the prominent $A\ ^3\Pi_{1u}$ wave-packet peak at low energy. The peak at ~840 meV is consistent with two-photon absorption and subsequent dissociation into the atomic fragments $I(^2P_{3/2})$-$I(^2P_{1/2})$, which would give rise to an observed energy of ~758 meV at a delay of 20 ps [18]. The peak at ~1320 meV arises from two-photon excitation and subsequent dissociation into the $I(^2P_{3/2})$-$I(^2P_{3/2})$ channel (expected energy position ~1226 meV) or three-photon excitation and subsequent dissociation into the $I(^2P_{1/2})$-$I(^2P_{1/2})$ channel (expected energy position ~1274 meV). We note that the energies of the observed peaks tend to be slightly larger than the expected energies of the two- or three-photon excited wave packets. This is consistent with Raman redistribution, discussed in Sec. IV B or with space charge effects (discussed in Sec. V).

No other two- or three-photon absorption channels can produce wave packets with dissociation energies close to the ones observed. Still, higher-order photon absorption processes might create wave packets, dissociating into highly excited atomic iodine states, that could account for part of the observed peaks.

In general, the presence of higher-order channels such as two- or three-photon excitation processes caused by the pump pulse adds a background to the pump-probe signal. At the 20-ps delay, where the Coulomb energy is very small, the wave-packet peaks, corresponding to the different dissociation energies, are clearly separated. However, at the smaller delays this is no longer the case since the sum of the Coulomb energy and the dissociation energy of the different wave packets might result in almost the same observed kinetic energy. For instance, at a delay of 0.5 ps, projection of the two-photon excited $I(^2P_{3/2})$-$I(^2P_{3/2})$ wave packet onto an I^+-I state gives rise to a kinetic energy of ~1213 meV whereas the projection of the $A\ ^3\Pi_{1u}$ wave packet onto an I^+-I^+ state results in a kinetic energy of ~1170 meV. These energies are not resolvable in our experiment and cause the relatively broad structure of the I^+-I^+ peaks observed at a delay of 0.5 ps (Fig. 3). Thus, the presence of multiphoton excited wave packets enhances the width of the experimental internuclear distributions at the 0.4-, 0.5-, and 0.6-ps delays and is one reason for the difference between measurement and simulation in Fig. 4.

Although in our experiment two- and three-photon excitation transitions are clearly observable in the 20-ps delay spectrum, such multiphoton processes can be significantly suppressed by lowering the intensity of the pump pulse. The single-photon excitation probability will be reduced, but the experimental signal-to-noise ratio can still be excellent if high repetition rate ($\geq$kHz) lasers are used.

B. Raman redistribution of vibrational population

Another nonlinear interaction that can influence the formation of the wave packet is stimulated Raman transitions. Since the bandwidth of the pump pulses (~32 meV) is larger than the vibrational level spacing (~26 meV) in the ground electronic state of I_2, part of the population in an initial vibrational level might be transferred to a higher-lying vibrational level by a stimulated Raman transition. Thus, the initial Boltzmann distribution of vibrational levels might be redistributed by one or several Raman processes thereby adding vibrational energy to the I_2 molecule. This would manifest itself as additional dissociation energy of the wave packet. The I^+-I peaks, which reflect the distribution of dissociation energies, are located around ~238 meV and have a FWHM ~98 meV. In comparison, a wave packet excited from the $\nu=0$ level will be centered around 221 meV and have a FWHM equal to the laser bandwidth (~32 meV). Excitation of the small fraction of the Boltzmann distribution that initially resides in higher-lying vibrational levels (see Sec. II) adds some dissociation energy to the wave packet [19], but it is not sufficient to explain the observed distribution of dissociation energies.

We would like to stress that even though the observation of enhanced dissociation energies is consistent with stimulated Raman transitions redistributing the vibrational population a significant contribution to the broadening of the I^+-I peaks towards higher energies will come from space charge effects (Sec. V). However, Raman transitions should always be considered as a potential interaction mechanism in studies with high intensity and short duration laser pulses [20,21].

We also observe dissociation energies smaller than what is possible for a laser bandwidth limited excitation of the wave packet from the $\nu=0$ level. This is due to the finite energy resolution of our ion TOF spectrometer, which always broadens the peaks towards smaller energies. The broadening is estimated to ~30 meV (Sec. II) in reasonable agreement with the observation of ~197 meV at the low-energy point where the amplitude of the I^+-I peaks in Fig. 3 is reduced to 50% of the maximum value.

In the deconvolution procedure, described in Sec. III, we used a functional form of the distribution of dissociation energies. This was obtained by fitting a Gaussian function to the I^+-I signal for energies $\geqslant$221 meV, thereby modeling the effect of the possible population redistribution and space charge effects. For energies $\leqslant$221 meV we simply replaced the distribution function by another Gaussian function with a width equal to the bandwidth of the pump laser pulse. The limited energy resolution of the ion spectrometer and the possible influence of space charge effects on the I^+-I peak prevent this signal from being a perfect image of the actual distribution of dissociation energies. However, once these problems are removed, recording of the I^+-I signal will be an accurate way to determine the distribution of dissociation energies, necessary for the deconvolution procedure. In particular, this eliminates the need for a detailed knowledge of the Franck-Condon overlaps between the vibrational levels of the ground and the final electronic state ($A\ ^3\Pi_{1u}$), which would otherwise be required for a calculation of rather than an experimental determination of the distribution of dissociation energies.

C. Wave-packet dynamics of molecular ionic states induced by intense pump pulses

Rather than decreasing the intensity of the pump laser to suppress nonlinear effects in the excitation process, one can utilize the ability to efficiently drive high-order multiphoton absorption processes with intense femtosecond pulses to populate and initiate dynamics in ionic molecular states. Furthermore, it is possible to perform time-resolved spectroscopy of such states by using delayed femtosecond probe pulses to follow their evolution. For instance, we have recently employed an intense femtosecond pulse to efficiently excite a wave packet in an I_2^{2+} state, dissociating into the fragments I^{2+}-I [12], with the purpose of verifying the existence of a critical internuclear distance where the ionization rate of molecular ions is strongly enhanced [4]. In order to create the I_2^{2+} wave packet, the I_2 molecules absorbed an energy from the intense laser field equivalent to $\geqslant$16 photons at 625 nm. This experiment illustrates the approach of utilizing wave-packet technology [22] to study a new problem.

Along the same lines, we recently demonstrated that irradiation of molecules with intense femtosecond pulses provides a means of producing metastable molecular trications [23]. Thus, it was shown how Cl_2^{3+}, Br_2^{3+}, and I_2^{3+} can be formed by exposing the respective neutral halogen molecules

to an intense ($\sim 3\times 10^{14}$ W/cm^2), 80-fs-long optical pulse. The strong field facilitates the triple ionization while the short duration prevents the molecule from dissociating on transient potential curves during the ionization process.

To exert control of the outcome of the nonlinear processes driven by the pump pulse it will be advantageous to use laser beams with a constant spatial intensity profile. Presently, Gaussian shaped beams are employed with the result that, within the focal volume, a variety of different states are excited depending on the maximum intensity reached at a particular position in the focus. Since the signals recorded in our experiment represent an average over the entire focal volume, they consist of contributions from all states excited. Using a laser pulse with an essentially flat spatial profile should ensure a more selective state excitation. This will make the interpretation of the signals easier and increase the population transfer to desired states. A constant transverse intensity profile is achieved, for instance, by selecting the central part of a Gaussian beam with an undersized pinhole and imaging it. In the longitudinal direction the constant intensity is obtained by restricting the laser-molecule interaction to a dimension much smaller than the Rayleigh length.

We note that a constant spatial intensity profile will also be useful for the probe pulses employed to Coulomb explode the molecule. Here, it should ensure that a wave packet under study is projected primarily onto one type of charge state rather than onto a number of different charge states.

V. SPACE CHARGE EFFECTS

Space charge can influence the velocity distribution of ions when a focused laser beam ionizes a sample of neutral molecules or atoms. Most of the photoelectrons exit the focal region very rapidly, leaving behind a positively charged core of ions. The electrostatic interaction between the positive ions changes their energy spectra and angular distributions. In particular, the kinetic energy of the ions is expected to increase due to the repulsive force between them. Our experimental results are consistent with space charge in the velocity mismatch between the observed and the simulated wave packet (Fig. 4).

We can approximate the influence of space charge on the velocity distribution in the analysis of the kinetic energy spectra by assuming that it adds a constant value, E_{so}, to the observed kinetic energies: $E_{kin}=E_{Coul}+E_{dis}+E_{sc}$. Repeating the deconvolution procedure with E_{sc} as a free parameter, we obtain a much better agreement between the simulated and the observed internuclear distributions (Fig. 5) for E_{sc} equal to 50 meV.

Another indication of space charge comes from the position of the two high-energy peaks, in the 20-ps spectrum, resulting from the wave packets excited after two- or three-photon absorption. The observed energy positions of these peaks are $\sim$50–100 meV larger than the calculated kinetic energies of the respective channels (see Sec. IV A). This is in accordance with the value of E_{sc} determined in Fig. 5.

Space charge may also influence the I^+-I peaks. The effect should be smaller than in the case of the I^+-I^+ peaks since the I^+-I signal mainly originates from parts of the laser focus where the intensity is lower [24] and therefore where the charge density is lower. Nevertheless, the effect is consistent with the broadening of the I^+-I peaks towards higher energies.

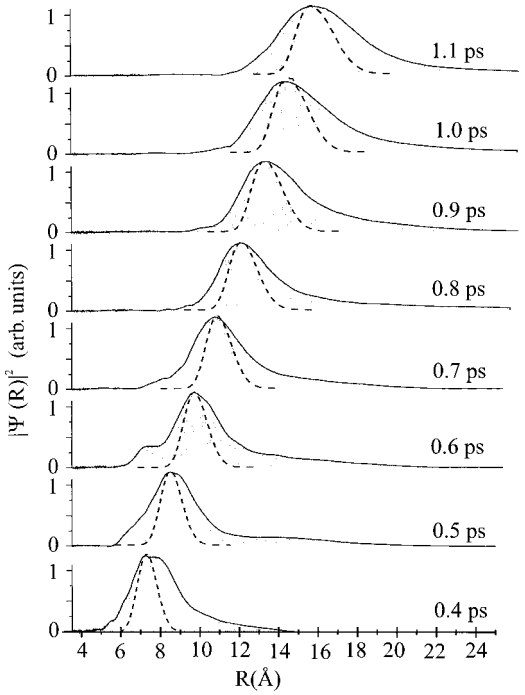

FIG. 5. Same as Fig. 4 except that space charge effects are taken into account in the analysis of the data by assuming that they add 50 meV of kinetic energy to the observed I^+ ions (see text for details).

We can estimate the space charge energy acquired by the ions in the laser focal volume following the ideas of Ammosov *et al.* [25]. The laser focus is approximated by a cylinder with a radius of ω_0 and length l. The electrons are assumed to exit the focal volume instantly, leaving behind a positively charged volume of approximately uniform charge density, αne, where α is the degree of ionization of each molecule, n is the density of molecules, and e is the elementary charge. As the cloud of ions expands due to Coulomb repulsion the I^+ ions gain a maximum energy of Ue, where U is the electrostatic potential felt by the ions at the surface of the cylinder. Since the length of the cylinder, approximately two times the confocal parameter, $2\omega_0^2/\lambda$, is much larger than ω_0, U can be calculated by Gauss's theorem: $Ue=\omega_0^2\alpha ne/2\varepsilon_0$, where ε_0 is the vacuum permittivity. Inserting the experimental values of ω_0 (12.5 μm) and n (6×10^{10} cm^{-3}), and assuming $\alpha=2$ (the I^+-I^+ channel is the dominant one), we obtain $Ue=170$ meV. The agreement with the experimental value of 50–100 meV is satisfactory in light of the simplicity of the space charge model and the uncertainty on the estimate of the density in the molecular beam. Thus, the outcome of the simple calculation corroborates the experimental indication of the non-negligible role of space charge. If high spatial resolution is required future Coulomb explosion experiments should be performed at lower gas density or with a small focal volume.

VI. ULTIMATE SPATIAL RESOLUTION LIMIT

Presently, the spatial resolution of the Coulomb explosion method to measure the size of wave packets is limited by the space charge and the energy resolution of the ion TOF spec-

trometer. Still, Fig. 4 demonstrates a spatial resolution of 2–4 Å for internuclear separations in the range 7–14 Å. Since both effects become more important as the energy of the detected ions decreases, the spatial resolution gets worse for large internuclear distances. However, our spatial resolution is not limited by fundamental physics. The pronounced broadening of the internuclear distributions towards large values for the larger delays (0.8–1.1 ps) is caused by the energy resolution of the TOF spectrometer. This can be improved by a better design of the spectrometer and space charge can be overcome by lowering the target density.

The ultimate resolution limit of our Coulomb explosion technique for measuring wave functions is determined by the effective duration of the probe pulse. The motion of the nuclei during the probe pulse leads to a blur of the measured internuclear position approximately equal to the product of the internuclear velocity and the effective pulse duration. This effective pulse duration is expected to be only a fraction of the real duration since the multiple ionization only occurs efficiently around the peak intensity of the probe pulse. In our experiment, the wave packet velocity of $\sim$11.6 Å/ps and the 80-fs-long probe pulse should therefore result in an ultimative spatial resolution better than 11.6×0.080 Å $\sim$0.9 Å. The development of high power pulses of 5–10-fs duration [26] will significantly improve the spatial resolution. Thus, measurements of wave-packet structure with a resolution of a few tenths of an Å seem feasible even for fast internuclear motions (10–40 Å/ps).

VII. OUTLOOK

So far we have only considered the measurement of wave packets at relatively large internuclear separations ($R \geqslant 6$ Å). This approach ensures that the probe pulse projects the wave packet onto a state that is purely Coulombic. However, at smaller internuclear separations some of the potential curves of molecular ions deviate significantly from a Coulombic shape. For instance, many molecular dications and trications exhibit metastable states [23,27,28]. In order to perform wave packet measurements at small internuclear distances, of the precision that we have described, it will be necessary to remove enough electrons from the molecule by the probe pulse that the Coulomb repulsion between the resulting atomic ions far exceeds the binding energy of the molecular ion in the absence of Coulomb repulsion. Ideally, the probe pulse should then remove all valence electrons. This can be readily achieved when the molecule consists of atoms with only one or two electrons in the valence shell such as alkali dimers or trimers. For molecules with a larger number of valence electrons, like I_2, explosion into highly charged atomic fragments will be required to ensure that the released kinetic energy approximately corresponds to the Coulomb energy [29].

One concern about using highly charged atomic ions is that the molecule is likely to pass through highly repulsive states during the removal of the electrons. If the probe pulses are too long, the internuclear motion on the transient repulsive potential curves will cause a deterioration of the spatial resolution. Thus, observing wave-packet motion at small internuclear separations will require the use of very short, $<$20 fs, probe pulses. In addition, as pointed out in Sec. VI, the nonlinear character of the transition to the highly charged molecular ions implies that the probe process only occurs efficiently during a fraction of the pulse duration corresponding to the highest intensities. This should minimize the effect of internuclear motion during the probe pulse and enable studies with a time resolution better than the actual duration of the probe pulse.

One obvious goal in future work is to extend time-resolved Coulomb explosion imaging from studies of diatomic molecules to studies of polyatomic molecules. In the case of polyatomic molecules laser-induced Coulomb explosions holds the promise to directly observe three-dimensional evolutions of the nuclear configuration. This is an intriguing subject and one that is not yet well addressed by femtosecond spectroscopy. We note, however, that observing three-dimensional structures is a problem that has been confronted, for instance, in beam-foil non-time-dependent Coulomb explosion studies [5,6] and various other fragmentation type experiments [30]. This has led to the development of advanced three-dimensional imaging methods which should be applicable in the laser-induced studies.

Timed Coulomb explosion imaging will not provide as precise values for spectroscopic constants as more traditional spectroscopy methods but wave packet studies are unlikely to require such precision. Optically driven Coulomb explosion imaging may have applications in addition to observing molecular dynamics. The technique is very simple and compatible with molecular beam or ion beam technology. It has a significant advantage over spectroscopy in not requiring any *a priori* model for the molecules under study because the technique gives direct information about the molecular geometry. Thus, Coulomb explosion imaging could be of particular importance for the study of floppy molecules encountered in highly excited states of most molecules or in the case of van der Waals molecules.

VIII. SUMMARY AND CONCLUSION

Femtosecond laser-induced Coulomb explosion imaging is a new method to study dynamics and structure of molecules on a natural temporal (fs) and spatial (Å) scale for molecules. It is based on initiating internuclear motion with a femtosecond pump pulse and measuring the time-dependent internuclear position and shape by Coulomb exploding the molecule with an intense, delayed probe pulse. To test the performance of the technique it was applied to study photodissociation of iodine molecules. We measured the wave function of I_2 molecules dissociating in the $A\ ^3\Pi_{1u}$ potential with a resolution of 2–4 Å in the internuclear range of $\sim$7–14 Å. When space charge effects, present in our experiment, are eliminated and the energy resolution of the ion spectrometer is improved it seems feasible to reach the ultimate spatial resolution limit given by the product of the internuclear velocity and the effective duration of the probe pulse. This effective pulse duration is smaller than the real duration due to the high nonlinearity of the probe process. Thus, the future use of probe pulses of 5–10 fs duration should make it possible to perform time-resolved studies of internuclear structure with a spatial resolution of a few tenths

of an Å and a time resolution of the order of the optical period of the probe pulse.

Highly nonlinear interactions such as multiphoton ionization not only provide a method for probing molecular dynamics but it can also be employed to initiate dynamics. Finally, it should be possible to follow photochemical events taking place in polyatomic molecules with the goal of measuring three-dimensional structural changes on an ultrafast time scale.

ACKNOWLEDGMENTS

We would like to acknowledge the technical support from D. Joines and the help and advice from A. Stolow.

[1] *Proceedings of the Conference on Ultrafast Phenomena IX*, edited by P. F. Barbara, W. H. Knox, G. A. Mourou, and A. H. Zewail (Springer-Verlag, Berlin, 1994); *Proceedings of the Conference on Ultrafast Phenomena X*, edited by P. F. Barbara, J. G. Fujimoto, W. H. Knox, and W. Zintu (Springer-Verlag, Berlin, 1996).

[2] So far there exists no condensed phase analog.

[3] S. Augst, D. D. Meyerhofer, D. Strickland, and S. L. Chin, J. Opt. Soc. Am. B **8**, 858 (1991).

[4] T. Seideman, M. Yu. Ivanov, and P. B. Corkum, Phys. Rev. Lett. **75**, 2819 (1995).

[5] Z. Vager, T. Graber, E. P. Kanter, and D. Zajfman, Phys. Rev. Lett. **70**, 3549 (1993).

[6] Z. Vager, R. Naaman, and E. P. Kanter, Science **244**, 426 (1989).

[7] H. Stapelfeldt, E. Constant, and P. B. Corkum, Phys. Rev. Lett. **74**, 3780 (1995).

[8] G. M. McClelland, K. L. Saenger, J. J. Valentini, and D. R. Herschbach, J. Phys. Chem. **83**, 947 (1979).

[9] *Atomic and Molecular Beam Methods*, edited by G. Scoles (Oxford University Press, Oxford, 1988), Vol. I, Chap. 2.

[10] P. Dietrich, D. T. Strickland, M. Laberge, and P. B. Corkum, Phys. Rev. A **47**, 2305 (1993).

[11] R. J. Oldman, R. K. Sander, and K. R. Wilson, J. Chem. Phys. **54**, 4127 (1971).

[12] E. Constant, H. Stapelfeldt, and P. B. Corkum, Phys. Rev. Lett. **76**, 4140 (1996).

[13] A small fraction of the dissociating molecules are expected to be projected onto an I^+-I^{2+} potential. However, the low collection efficiency of I^+ ions resulting from this channel makes the observation difficult.

[14] A chirped pump pulse is not dealt with in this paper.

[15] J. Tellinghuisen, J. Chem. Phys. **58**, 2821 (1973).

[16] At a wavelength of 625 nm there is also a small probability that the $^1\Pi_u^+$ potential of I_2 is excited [15]. This is not included in the simulation since the dissociation dynamics of a wave packet launched on the $^1\Pi_u^+$ potential will be essentially identical to one launched in the $A\ ^3\Pi_{1u}$ potential.

[17] In fact, even some ionization of I_2 is observed when only the pump pulse is applied.

[18] Actually, the Coulomb energy is not completely negligible at a delay of 20 ps. This is taken into account in the calculation of the predicted positions of the peaks, assuming that the I^+-I^+ explosion channel is the dominant one.

[19] The exact shape of the wave packet will not only depend on the population in the vibrational levels but also on the Franck-Condon overlaps involved in the excitation.

[20] A. M. Weiner, D. E. Leaird, G. P. Wiederbrecht, and K. A. Nelson, Science **247**, 1317 (1990).

[21] L. D. Noordam, H. Stapelfeldt, D. I. Duncan, and T. F. Gallagher, Phys. Rev. Lett. **68**, 1496 (1992).

[22] I. Sh. Averbukh, M. J. J. Vrakking, D. M. Villeneuve, and A. Stolow, Phys. Rev. Lett. **77**, 3518 (1996).

[23] H. Sakai *et al.* (unpublished).

[24] P. Dietrich, D. T. Strickland, and P. B. Corkum, J. Phys. B **26**, 2323 (1993).

[25] M. V. Ammosov, F. A. Ilkov, M. G. Malakhov, and Ch. K. Mukhtarov, J. Opt. Soc. Am. B **6**, 1961 (1989).

[26] M. Nisoli, S. De Silvestri, and O. Svelto, Appl. Phys. Lett. **68**, 2793 (1996); M. Nisoli *et al.*, Opt. Lett. **22**, 522 (1997).

[27] P. J. Bruna and J. S. Wright, J. Phys. B **26**, 1819 (1993).

[28] G. Handke, F. Tarantelli, A. Sgamellotti, and L. S. Cederbaum, J. Chem. Phys. **104**, 9531 (1996).

[29] C. P. Safvan and D. Mathur, J. Phys. B **27**, 4073 (1994); D. Mathur *et al.*, *ibid.* **26**, L141 (1993).

[30] J. Becker, K. Beckord, U. Werner, and H. O. Lutz, Nucl. Instrum. Methods Phys. Res. A **337**, 409 (1994).